PFC/JA-87-7

Cusp Stabilized Mirror Based Neutron Source

J. Kesner, S. F. Horne, and V. P. Pastukhov*

July 1987

Plasma Fusion Center
Massachusetts Institute of Technology
Cambridge, Massachusetts 02139 USA

Submitted to Journal of Fusion Energy.

Supported by United States Department of Energy Contract DE-AC02-78ET51013.

*Present address: I. V. Kurchatov Institute, Moscow, USSR.

ABSTRACT

An optimally sized Fusion Engineering Test Facility should produce 10-20 MW of power at 2 MW/m^2 steady state wall loading. Because Mirror cells do not scale with size one can choose the fusion power and wall loading free from minimum size constraints. A cusp stabilized axisymmetric mirror is seen to be ideally suited for this purpose due to excellent access, a simple coil set and good MHD properties. We present parameters for a proof of principle experiment as well as for a Neutron source facility.

I. Introduction

Neutron Source requirements, Tokamak vs. Mirror

As fusion approaches the goal of a demonstration power plant both the physics and engineering must be developed in a timely and coordinated fashion. It is widely believed that a Tokamak can satisfy the constraints imposed by both physics and engineering and lead to a desirable power producing reactor.

There are several plausible paths toward the commercial application. One suggested critical path would include simultaneously a physics test experiment (similar to the proposed Compact Ignition Experiment, CIT) and an engineering component test experiment (termed FERF). These devices would be followed by an Engineering Test reactor (ETR). A second critical path would eliminate the FERF thereby reducing near term costs. The FINESSE study [1] rated the former critical path as most desirable. Although the near term funding requirements are higher , the overall funding requirements are comparable and overall operational risk and nuclear testing/development risk are significantly reduced.

Although nonfusion neutron sources will play a role in materials development component testing requires that these tests be performed in a fusion environment [1,2]. The fusion environment encountered by nuclear components involves the simultaneous presence of neutrons, high magnetic fields, tritium, surface and bulk heating, vacuum, and radiation and particle surface bombardment. Fission reactors and point neutron sources can play a significant role in the engineering development of fusion, but spectral differences, inadequate volume and inability to simulate the combined environment dictate the necessity for a fusion based neutron producing facility.

The requirements for this facility have also been considered by the Technical Planning Activity, known as TPA[2]. Table I reproduces the TPA findings. The requirements for this facility can be summarized as follows:

1. Component test area $>$ 5 to 10 m^2 with Neutron Wall Loading of $>$ 2 MW/m^2.

   Thus the desired fusion power output is in the range of 10 to 20 MW.

2. Steady State or Near Steady state (t $>$ 500 sec.) operation.

3. High Fluence. Lifetime Fluence $>$ 4-10 $MW \times yr/m^2$.

4. Tritium requirements that do not exceed existing supply to avoid dependence on breeding for operation.

Item 4 implies that tritium requirement not exceed $\approx$ 3 kg of tritium/year (the total amount that is available from the Canadian Fission Reactor Program). This limits fusion power production to $\approx$125 MW. This constraint is consistent with item 1 which implies an optimum machine power of below 20 MW. For such a device we would be assured of the availability of fuel and have a sufficiently large region of high neutron flux for component testing, notably for tritium breeding blanket modules. Skipping the FERF step would undoubtedly reduce the ETR availability. Since the required quantities of Tritium are unavailable, it must breed its own fuel using a technology which is itself under development.

One option for a FERF device would utilize a Tokamak. A Tokamak engineering device is credible and can be viewed as supporting the development of the Tokamak physics data base. At present Tokamaks appear to exhibit the best confinement of any fusion device. They have a large data base and strong international collaboration. It appears that the next generation of these devices can ignite and can make viable power producing reactors.

However, it has been shown that the fusion power for ignited tokamaks must exceed 150 and possibly 200 MW. Although this relatively large power translates into a large test area the the wall loading in the test area tends to be marginal ($\approx$1 MW/m^2) and the useful test area is limited to the outer part of the torus. The high fields required in these devices further limit access and the use of normal coils to produce high fields with minimal shielding results in high associated electricity costs.

Small tokamaks can also be run as unignited driven devices. Here again the limited access in the inner part of the torus is a constraint. High fusion power density favors beam-plasma operation. Additionally beta limitations favor reduced confinement [3] so that energetic particles will be lost after they slow down (and their reactivity drops). Optimal power density thus favors operation in a mirror-like confinement regime in which hot ion confinement is limited to an electron drag time. Additionally small tokamaks tend to have relatively short pulse operation.

Another option for an engineering test facility would be to use a mirror device to simulate tokamak reactor conditions. Confinement in single mirror cells is limited by velocity space pitch angle scatter and as a result it is difficult to produce Q $>$ 1 in these devices (Q is the ratio of fusion power produced to input power into the device). Attempts to improve confinement have led to the development of multi-cell electrostatically plugged tandem mirrors.

Unplugged mirrors are however ideal for neutron producing devices. The advantages of a mirror based device over a toroidal device are as follows:

1. No Scaling with size. We will show that a 10 MW device is entirely plausible.
2. Inherently steady state.
3. Cylindrical geometry. This eliminates the poor access into the inner 2/3 of a small aspect ratio torus.
4. No density limit dictated by physics. The density limit is set by the requirements for neutral beam penetration.

Several studies have been performed on mirror based neutron sources, including MFTF-ALPHA+T [4], TDF [5], TOSKA-M [6] and they confirm these conclusions.

An energetic research effort, including a strong international cooperation with Japan and the USSR has produced significant progress. MHD stability has been obtained through the use of minimum-B mirror cells that can be linked to axisymmetric cells. Microstable hot ion populations have been created in both quadrupople and axisymmetric mirror cells through the use of tailored beam-injected ion distribution functions. Furthermore it has been observed that the only MHD instability observed in a tandem mirror is the "rigid" m=1 mode, presumably due to the strong FLR stabilization present in these devices for m> 1 modes. Thus stabilization techniques need only deal with the m=1 mode [7].

Table II., reproduced from the FINESSE study [1], compares tandem mirror based neutron studies mentioned above with the Tokamak based devices FED-R(II)[8] and INTOR [9]. FED and INTOR have unacceptably high tritium consumption, marginal wall loading and a factor 2 higher capital and cumulative cost. Thus we conclude that a Tokamak is well suited for fusion power production while a mirror based device is better suited as a small , high fluence fusion engineering device.

Cusp Stabilized Neutron Source

During the last decade the mission of mirror fusion research was to produce a fusion reactor. The research was thus focused on developing techniques for producing high confinement and substantial attention was directed to end plugging and thermal barriers as a means of confinement enhancement. In their simpler form (without thermal barriers), mirror based devices are ideally suited for neutron production. In this role confinement enhancement becomes unimportant and a Q value of 10 % is quite acceptable. In considering a mirror based device in this light, the question that must be addressed is the ability of these devices to scale up in density and temperature while maintaining MHD and microstability.

Axisymmetric devices are particularly interesting for this purpose. Axisymmetry pro-

vides excellent access and uniform illumination for the testing modules in the neutron producing cell (which we will term the target cell). Furthermore axisymmetric coil design permits higher fields to be generated by simpler and more efficient coils which results in a reduction of the beta and therefore the target cell instability drive. Additionally axisymmetry reduces radial transport.

While the programmatic orientation in the mirror program toward a high confinement device has produced important advances in understanding mirror physics, schemes that do not appear to have reactor potential were not vigorously pursued. One particularly interesting geometry is a cusp stabilized axisymmetric device. Cusps received only modest attention during the last decade due to the fact that loss of adiabaticity near the axially located field null was known to result in poor confinement in this region. However although this loss produces an unacceptable degradation of confinement for a high confinement device, it is not a significant problem in a low confinement neutron production facility. Recent experimental results in the RFC-XX device [10] has rekindled interest in cusps. Two new cusp based experiments are being planned in the USSR , one is a cusp stabilized tandem mirror designed by Dimov et. al.[11] in Novosibirsk and the second a smaller facility designed by the Ioffe group in the Karchatov Institute.

The cusp has several important advantages over other mirror devices.

1. It is axisymmetric, and is produced by a particularly simple coil set.
2. It possesses very good stability properties.
3. The mirror ratio to the line cusp can be large (R $\approx$ 5 to 10) which decreases the velocity space hole ($\propto \phi$ /(R-1)). This will reduce the drive for microinstability in the energetic cusp confined species.

Fig 1. shows a prototype magnetic field geometry for such a device. The midplane located "target cell" is axisymmetric and it is here that sloshing neutral beams are injected to form a localized region of high fusion density. The fueling cells which flank the target cell produce the target plasma for beam start-up and for either neutral beam or ICRF trapping in the outboard cusp anchors. Stability requirements for the device will be treated in the next section.

In section 2 we will review stability requirements for the proposed geometry. Section 3 presents an illustrative example of neutron source parameters. Section 4 discusses fueling of the target cell and section 5 contains parameters for a proof-of-principle experiment. Section 6 contains concluding remarks.

II. Cusp Stabilization

Consider a spindle cusp arrangement shown in fig. 1. The flux tube exiting the target cell maps through cusp cells located on each end of the device. Since the radius curvature in the cusp is comparable with the field line radius ,i.e. the cusp is not long-thin, stability derives from both the usual curvature ($\propto 1/ R_c$,with R_c the radius of curvature) and the compressibility ($\propto 1/ R_c^2$). A cusp can thus be strongly stabilizing to m=1 "rigid" modes (m is the azimuthal mode number).

A critical issue with a cusp cell is the loss of adiabaticity in the vicinity of the field null. This will produce a positive radial pressure gradient in the vicinity of the axis which can drive radially localized MHD instabilities. Stability of these modes require that there be enough streaming plasma in the vicinity of the axis for compressibility and rotation to balance the instability drive from the positive pressure gradient. Additionally these short wavelength modes can be strongly stabilized by Finite Larmor Radius (termed FLR) effects.

From the MHD formulation, a sufficient condition for stability of the m=1 mode is

$$\begin{aligned} \delta W &= \int \psi d\psi \left(p'U' + \gamma p (U')^2/U\right) \\ &= \int \psi d\psi \frac{U'}{U^\gamma} (pU^\gamma)' \\ &= \int d\psi p U^\gamma \left(\frac{\psi U'}{U^\gamma}\right)' \end{aligned} \tag{1}$$

with U = $\int$ dl/B and the primes represent the flux (ψ) derivative.

Recalling that

$$\frac{dU}{d\psi} = -2 \int \frac{dl}{B^2 r Rc} \tag{2}$$

with R_c the vacuum field line radius of curvature we see that the first term is the curvature drive and the second the compressibility.

A simple analytic model for an "ideal" cusp is

$$\psi = \frac{1}{2} C r^2 z \tag{3}$$

If we assume that pressure is constant within a mod-B surface defined by B = B_o and that the two crossings of the mod-B surface by the field lines occur near to the axis and the

cusp midplane respectively we can solve for U and find

$$U = C\ln(\hat{\psi}/\psi) \tag{4}$$

with $\hat{\psi}= 2C^2B_o^3$. Notice U has a logarithmic singularity at $\psi = 0$. We see from the second form of eq. 1 that moving towards the axis the pressure must decrease slower than $U^{-\gamma}$. A less restrictive condition obtained from CGL theory [12] would permit $p \propto r^{\gamma}$.

We have found that eq. 4 is in fact an excellent approximation for U for realistic coil configurations. Thus for a given coil set we can determine C and $\hat{\psi}$ and then use a model pressure profile to integrate eq. 1.

We can also use Eq. 4 to calculate the volume within a mod-B surface. If the mod-B surface extends out to the flux tube defined by the target cell flux, $\psi = \psi_{\max}$, we obtain

$$V = 2\pi C\psi_{\max}(1 + \ln(\hat{\psi}/\psi)) \tag{5}$$

In comparing cusp cells it is useful to use as a figure of merit δW / V since a larger volume implies more power input to maintain a given pressure.

For a parabolic target cell pressure profile and a model hollow cusp cell pressure profile of the form

$$P(\psi) = 6.75P_{\max}\left(\frac{\psi}{\psi_{\max}}\right)^2(1 - \psi/\psi_{\max}) \tag{6}$$

we obtain the requirement

$$\frac{P_{\text{cusp}}}{P_{\text{target}}} > \frac{\psi_{\max}}{C_1 L_t B_t^2} \tag{7}$$

with

$$C_1 = 6.75\,\gamma C\int_0^1 \frac{x\,dx\,(1-x)}{\ln(x\hat{\psi}/\psi_{\max})}$$

L_t is the transition length of the target cell and B_t the target cell field.

III. Neutron Source Parameters

The primary mission of a fusion based neutron source facility is component testing in a simulated Tokamak environment. We use the results of the Technical Planning Activity results displayed in Table I to define the desired parameters for an engineering test facility. In particular we would like to achieve the following parameters:

Neutron flux > 1.5-2 MW/m^2

Test area of 5-10 m^2.

Pulse length > 30 sec.

In approaching the design of such a facility several important constraints must be satisfied. They are as follows:

1. Beam penetration. For Tritium at ≈150 KeV requires $<n_eL> < 8x10^{15}$.
2. Magnet design. A reasonable maximum mirror field of 12-15 T.
3. Confinement of sloshing Tritium Beams. Neutron source Vacuum mirror Ratio > 2.5. This implies $B_{vac} \approx 5$ T.
4. MHD Stability. Mirror equilibrium studies indicate maximum beta in axisymmetric neutron source cell should not exceed 50 %.

We consider the case of energetic Tritium neutral beams injected into a Deuterium target. (The target may be fueled with low energy Deuterium neutral beams). To evaluate tritium confinement we will use the Logan-Rensink analytic model [13] (derived from Fokker-Planck simulations). To minimize the drive for ion loss cone microstability we assume the electron temperature remains low (< 2 Kev). As a result of the low electron temperature Tritium confinement is dominated by electron drag.

For energetic ions dragging on electrons the ion distribution function can be approximated by

$$f_T = \frac{n_e}{\ln(\frac{v_{inj}}{v_{loss}})} \frac{1}{v^3} \tag{8}$$

for v_{inj} the injection velocity and v_{loss} the loss energy. The logarithmic term is approximately 1. For beta limited confinement fusion power density can be written as

$$\begin{aligned} P_{fus} &= n_D n_t < \sigma v >_{DT} E_{fus} \\ &= \frac{\beta^2 B_{vac}^4}{8\pi} < \sigma v >_{DT} \frac{E_{fus}}{E_o^2} \end{aligned} \tag{9}$$

with E_{inj} the injection energy and E_o the mean hot ion energy and E_{fus} = 14.1 MeV, the neutron energy released per fusion. P_{fus} has a broad peak at an injection energy of 140 Kev for Tritium and rises strongly with beta and magnetic field. We can use beta and/or B_{vac} to push density to the limit set by beam penetration.

Beam penetration sets a limit on [n_e a]. The total fusion power per unit length, P_{tot} = P_{fus} × Vol / Length , rises with [n_e a] and with injection energy proportional to $< \sigma v >$,

$$P_{\rm tot} \; = \; \pi f(1-f)\,[n_e a]^2\; E_{\rm fus}\; < \sigma v >_{\rm DT} . \tag{10}$$

Here a is the plasma radius and f the fraction of Tritium (f = n_T/n_e). Thus for injection energies above the power density optimum the power per unit length will continue to rise although fusion power density begins to drop. The optimum configuration would thus utilize injection near 140 KeV and vary B_{vac} so that the plasma radius is limited by the beam penetration requirement.

The power amplification factor Q is defined to be the ratio of fusion power (counting 17.6 MeV per fusion event) to injected power. Since the injected current must balance ion losses

$$I_{\rm inj} \; = \; \frac{P_{\rm inj}}{E_{\rm inj}} \; = \; f\,\frac{n_e^2 V}{n\tau}, \tag{11}$$

we can combine eqns. 10 and 11 to obtain

$$Q \; = < \sigma V >_{\rm DT} \; n\tau\,\frac{E_{\rm fus1}}{E_{\rm inj}} \tag{12}$$

with E_{fus1} = 17.6 MeV. Q peaks at $E_{inj} \approx$ 212 KeV.

In order to maximize Q and optimize P_{fus} we will want injection energies at the upper end of the optimum fusion power density range and for the illustrative example shown in table III we choose $E_{inj} \approx$ 150 Kev. This energy also turns out to be at the upper end of the beam injection energies attainable with positive energy Tritium sources. From eq 12 we see that Q increases with increasing T_e (since $[n\tau] \approx [n\tau_{drag}] \approx T_e^{1.5}$).

For 150 Kev Tritium injection we can raise the vacuum field up to the limit for beam penetration. Since electron drag dominates ion confinement the electron temperature will determine Q as seen in eq. 12. Thus lower electron temperature requires more neutral beam current. For an example we can choose T_e = 2 KeV and obtain the parameters displayed in Table III.

We have chosen to inject high energy Tritium into a Deuterium target fueled by low energy beams (15 to 25 KeV). This is preferable to a high energy Deuterium scenerio because penetration of the lower energy component is aided if it is the lower mass species. The Tritium would be injected at a vacuum mirror ratio of ≈ 2 to produce a sloshing profile. The sloshing profile is maintained because the high energy beam is considerably dragged down in energy before pitch angle scatter takes place.

Deuterium fueling could be accomplished through the use of low energy beams or by pellet injection. Beam penetration and fueling issues will be discussed in the next section. Deuterium beams in the 15-25 Kev range would be sufficiently energetic to penetrate if injected near to the mirror throat. For either case the low energy Deuterium does not contribute substantially to the beta. Microstability could be provided by the electrostatic trapping of warm plasma within the potential well created by the sloshing Tritium and beyond the potential peak by the warm Deuterium that fuels the anchors.

In order to maintain the electrons at the low temperature assumed here and to satisfy an electron power balance requires a gas input into the source cell. Assuming that each electron-ion pair carries out 7 Te of energy, removal of the 92 MW of injected power requires 5.1 KA. of current to be injected between the target and anchor cells.

IV. Fueling of Target Cell

In the target cell we want to maximize neutron production subject to constraints on beta and on beam and pellet penetration. We have considered optimizing the device for 2 component, beam plasma fusions. For reasons discussed in sec. II we choose injection of $\approx$ 150 KeV Tritium beams into a target formed by 20 Kev deuterium beams.

The Tritium would be injected perpendicular to the machine axis at a vacuum mirror ratio of about 2 (the beta depressed mirror ratio is ≈ 2.6). At the modest electron temperature envisioned, 1 to 2 KeV, the tritium will drag down to about 30 Kev and then pitch angle scatter thus forming a sloshing population. Fig. 2 shows schematically the axial density profiles of Deuterium and Tritium within the target cell.

The Deuterium plasma component could be injected as pellets into the target cell potential well formed by sloshing Tritium or as low energy beams. We would like to keep the Deuterium pressure low so that Deuterium would not occupy significant beta. Pellet injection requires technology development in terms of producing sufficiently high velocity pellets to penetrate to the target cell axis. (This development may take place within the context of CIT). Studies have shown that penetration of the more tenuous TFTR plasma would require injection energies in excess of 20 Km/sec [14] which is well beyond current technology. We will consider below the injection of low energy deuterium beams.

Beam penetration is a critical issue for the lower energy deuterium beams. The beam density will e-fold in a distance (normalized to the local plasma radius) of

$$L_e/a(s) = \frac{v_b}{na < \sigma v >_{\rm eff}} \left(\frac{B_{\rm inj}}{B_c}\right)^{1/2} \tag{13}$$

The square root factor reflects that the flux tube narrows as the magnetic field rises. To obtain similar radial profiles for D and T we would like equal values of L_e / a. We require that the plasma radius be about L_e. For 150 KeV Tritium we obtain using rate coefficients from Table IV, $L_e \approx 7.2$ cm.

The 20 KeV Deuterons have a lower velocity than the energetic Tritons and thus are less penetrant. They can however be injected at a higher vacuum mirror ratio than the Deuterium where the flux tube has a smaller radius. Furthermore, Tritium density would be largely be absent at this location so n_e is reduced by a factor of ≈ 2. Table IV displays the relevant cross sections [15] at these energies. Notice that charge exchange is dominant for the 20 Kev beams but relatively unimportant for the 150 KeV T beams. Some fraction, α, of the charge exchange is reabsorbed in the plasma so that a fraction of the charge exchange can be considered as a source.

We can add the ionizing rate coefficients with $\alpha \times < \sigma v >_{cx}$ to obtain the total effective rate coefficient, i.e.

$$< \sigma v >_{\rm eff} = < \sigma v >_{ii} + < \sigma v >_{\rm ei} + \alpha < \sigma v >_{\rm cx} \tag{14}$$

For the energetic Tritium beams it is appropriate to replace the Maxwellian averaged $< \sigma v >_{\rm ii,cx}$ by the cross-section, velocity product. For these parameters we obtain the ratio of e-folding lengths to be $L_e(T)/L_e(D) \approx 1.4$. For comparable beam penetration the Deuterium beams must be injected at a 1.9 times the field of the Tritium injection. Assuming that beta is 30 % at the Tritium injection point but is small at the Deuterium injection point we find that the Deuterium beams must be injected at a vacuum mirror ratio of 3.2 . The total mirror ratio of the cell should be about ≈ 5 which implies a peak field of > 20 T.

These requirements can be relaxed if the Deuterium could be fueled by pellet injection into the sloshing-ion potential well. However pellet penetration is difficult in the presence of the energetic beam particles which can penetrate the dense cloud that will normally shield the incoming pellets. Calculations imply a required velocity of in excess of 20 Km/sec [14]. Although such injection speeds have been considered they would impose a challenging requirement on injector technology.

The need for higher peak fields that permit penetration of lower energy beams can be circumvented by the injection of Deuterium of equal velocity to the Tritium, i.e. at 100 Kev for the parameters discussed above. In this scenario the Deuterium is injected at the same mirror ratio as the Tritium and the peak field need only be about 3 B_o, that is 12 T. This would relax requirements on magnet technology but would result in a required reduction in the Tritium density of 60 % in order to produce the same beta. The reduced wall loading would be $\approx$ 1 MW/m^2.

V. Parameters for Proof of Principle Experiment

The proposed proof-of-principle experiment would provide a test of the following critical elements of this configuration :

1) Provide a quantitative comparison of the stabilization of a cusp anchor to m=1 MHD and Trapped Particle modes with theoretical predictions.

2) Quantify understanding of the stability of high m modes in the vicinity of the cusp null and the power loss from the cusp region.

3) Compare microstability of the sloshing hot ion target cell species with theoretical predictions. Theory predicts that high harmonics of ion cyclotron modes can be unstable [16] but these modes have not been experimentally observed.

4) Study microstability of the hot ions in the cusp.

The parameters of the beam injected species were calculated using a bounce-averaged Fokker-Planck code [17]. Typical parameters for such a device (termed Tara-N because of its similarity to the Tara device) are shown in Table III. The Axicell density is 1x10^{13} cm^{-3} with a mean energy of 5 Kev. This corresponds to injection of 150 A. with a confinement parameter $n\tau$ of 7x10^{10} sec/cm^3.

We have considered several cusp configurations. The three of primary interest, shown in Table V are 1) the inward facing cusp, 2) the symmetric cusp and 3) the outward cusp. Fig. 3 shows the flux mapping of these three arrangements.

For each design we have determined the stabilization properties assuming that the pressure is confined within a Mod-B surface that is tangent to the flux tube that maps into the target cell. To evaluate stability we use a pressure profile that is parabolic at the origin, i.e. P$\propto \psi^2(1\text{-}\psi/\psi_{max})$. Table V presents the results of this study. The outward facing cusp has weaker stabilization properties by about a factor of 2 to 3 compared to the inward or symmetric designs. The stabilization per unit volume is also shown in this table and exhibits this same trend.

Table V also lists the minimum ratio of the cusp to target cell pressure that is required for stability (eq. 7). The high value of this ratio attests to the excellent stability properties of the cusp cell. The outward facing cusp exhibits the weakest stabilization. Nevertheless the ratio calculated, 18, is substantial. The outward facing cusp, (case 1) is down by a factor 4 from the vertical cusp in case 2. However, when this number is normalized to volume (larger volume requires more power), this ratio is reduced to 2.

The outward facing cusp is however, preferable from an engineering point of view. The flux leaving the target and source cells is diverted toward the outside of the configuration and the cusp coils fit within a relatively small in radius vacuum vessel. The cusp to target cell pressure ratio is reduced in this design but is nevertheless large. Thus we chose this design for more detailed study.

VI. Conclusions

We have shown that a mirror based device has important advantages over a toroidal device for a small engineering test facility. Since in this role the requirements for confinement are reduced the as yet unproven physics associated with tandem mirror plugging can be avoided. In this context we have considered a cusp stabilized device because of its simple coil set and good MHD properties.

Acknowledgements

The author wants to thank K. Brau and J. Casey for help in the magnetic field calculations. This work was performed under U.S. DOE contract DE-AC02-78ET51013.

References

1. M. Abdou et. al. "FINESSE, A Study of the Issues, Experiments and Facilities for Fusion Nuclear Technology Research and Development," UCLA Reports UCRL-ENG-84-30 (1984) and UCLA-END-85-39 (1985).
2. C. Baker et. al., "Technical Planning Activity Final Report," Argonne Report ANL/FPP-87-1 (1987).
3. D. L. Jassby, Nucl. Fus. 15 (1975) 453.
4. K. I. Thommassen, J. N. Doggett, B. G. Logan and W. D. Nelson, "An Upgrade of MFTF-B for Fusion Technology," LLNL Report UCRL- 90825 (1984).
5. T. K. Fowler and B. G. Logan, "Tandem Mirror Demonstration Facility," LLNL Report UCID-19193 (1981).
6. B. Badger et. al., "TASKA-M A Low Cost, Near Term Tandem Mirror Device for Fusion Technology Testing," Uuiv. of Wisconsin Report UWFDM-600 (1983).
7. J.Irby et. al., "Experimental Study of Nonlinear m=1 Modes in the Tara Tandem Mirror", MIT Report PFC/JA-87-17, (1987), submitted to Physics of Fluids.
8. D. L. Jassby, S. S. Kalsi, Eds., "FED-R, A Fusion Engineering Device Utilizing Resistive Magnets," Fusion Engineering Design, Oak Ridge Report ORNL/REDC-82/1 (1983).
9. W. M. Stacy, "U.S.FED-INTOR Activity Critical Issues," Georgia Institute of Technology Report, FED-INTOR/TEST/82-2 (1982).
10. S. Horne, Manuscript in Preparation (1987).
11. G. I. Dimov and P. B. Lysyanskiy, "The AMBAL-M Ambipolar Trap," Inst. of Nuclear Sciences of the Siberian Division of the Academy of Sciences, Report 86-102 (1986).
12. V. P. Nagornyi and G. I. Stupakov, Sov. J. Plasma Phys. 10 (1984) 275.
13. B. G. Logan, A. A. Mirin, M. E. Rensink, Nucl. Fus. 20 (1980) 1613.
14. S. Milora, "New Algorithm for Computing the Ablation of Hydrogenic Pellets in Hot Plasmas," Oak Ridge Report ORNL/TM-8616 (1983).
15. R. L. Freeman and E. M. Jones, "Atomic Collision Processes in Plasma Physics Experiments," Culham Lab. Report CLM-R137 (1974).
16. M. Gerver, Private Communication (1987).
17. T. A. Cutler, L. D. Pearlstein, M.E. Rensink, "Computation of the Bounce Average Code, Report UCRL-52233 (1977).

TABLE 1 Nuclear Technology Test Facility

Purpose/Mission

Provide adequate environment for fusion testing of nuclear components.

Nature of Device

Any confinement concept that can provide a prototypical fusion environment with adequate test volume (5-10 m^3) can serve as the base facility. Options identified include tokamaks and mirror devices.

Key Features

Major Parameters	Parameter Values
Neutron wall load	1-2 MW/m^2
Surface heat load	0.2-0.5 MW/m^2
Plasma burn time	1000 s (steady state)
Plasma operating mode	Driven or ignited
Availability	30-50%
Fluence	2-3 $MW \cdot yr/m^2$
Test surface area	5-10 m^2
Fusion neutron power	< 100 MW

Major Design Features

Access to insert and remove test elements.
Sufficient space external to device to provide ancillary equipment supporting testing elements.
Component design compatible with test program.

Cost and Schedule

Options (based on a limited amount of design effort) have been defined. The PACE cost is on the order of a billion dollars.
Construction time would probably be five to six years.

TABLE II

Performance and Cost Comparisons of Verious Fusion Engineering Facility Candidates

	MFTF-α+T	TDF[a]	FED-R(II)	INTOR
Fusion power, MW	17	36	250	620
Neutron wall loading, MW/m^2	2.0	2.1	1.3	1.3
First wall radius, m	0.25	0.30	1.05	1.2
Component test area, m^2	1.6[b]	3.2	60	380
Ultimate availability, %	10	40	40	35
Limetime at ultimate availability, yr	10	10	10	10
Lifetime fluence, $MW=yr/m^2$	2.0	8.0	5.2	4.6

[a]Beam-fueled version.
[b]Can be increased to 3.2 m^2.

	MFTF-α+T	TDF	FED-R(II)	INTOR
Total capital cost, $M	400	1300	2100	2600
Electrical consumption, MW_e	150	250	600	300
Annual electrical cost, $M/yr[a]	7	44	105	46
Tritium consumption, Kg/yr	0.10	0.8	5.7	6.2[b]
Annual tritium cost, $M/yr[c]	2	16	115	124
Annual operating cost, $M/yr[d]	41	67	105	130
Total annual cost, $M/yr	50	127	325	300
Total cumulative cost, $M	~1000	~2800	~5700	~6000

[a]AT 50 mil/$KW_e h$
[b]Assumes INTOR TBR and blanket coverage of 50%.
[c]At 20,000 $/g.
[d]Estimate.

Table III

Target cell parameters

parameter	Proof of Principle	Neutron Source
Electron density(cm^{-3})	$2x10^{13}$	$6.7x10^{14}$ (n_T=$3.35x10^{14}$)
Plasma Length (m)	2	3.2
Plasma Radius (m)	.11	.12
solenoid Field (T)	.5-.7	4
Maximum B Field (T)	0.25	20
Flux (T-cm^2)	360	2000
Target cell beta (%)	3-6	40
Neutral Beam Voltage (Kev)	20	150 (Tritium) 20 (Deuterium)
Incident beam current (A)	140	548
Mean Ion Energy (KeV)	5	74
Electron temperature (KeV)	.2	2
Fusion Power		8.3
Neutron Flux (MW-m^{-2}) @ r=.25		1.8
Q (P_{fus}/P_{inj})		.13
$< n\tau >$ (sec/cm^3)		$8.4x10^{12}$
Area available for testing(m^2)		5

Table IV

Species	Energy KeV	$< \sigma v >_{cx}$ cm^3/s	$< \sigma v >_{ii}$ cm^3/s	$< \sigma v >_{ei}$ cm^3/s	$< \sigma v >^*_{eff}$ cm^3/s
D	20	10.6×10^{-8}	2.3×10^{-8}	1.8×10^{-8}	1.2×10^{-7}
T	150	$\sigma \times V$ 3.5×10^{-8}	$\sigma \times V$ 5.4×10^{-8}	1.8×10^{-8}	0.98×10^{-7}

* α=0.75

Table V

Case	1	2	3
Description	Outward	Vertical	Inward
C (cm/KG)*	6.5	13.3	59.2
$\hat{\psi}$(KG-cm^2)	1310	749	492
I1 (cm/KG)	6.2	19.9	130
Vol (l)	34	55	177
P_{cusp}/P_{target}	18	53	433

* $\int$ dl/B = C log($\hat{\psi}/\psi$)

Figure Captions

1. Schematic of magnetic field of a cusp stabilized mirror device.
2. Schematic of (a) magnetic field and (b) Tritium and electron density in target cell of neutron source.
3. Magnetic field geometry for (a) inward facing cusp, (b) symmetric cusp and (c) outward facing cusp.

CUSP STABILIZED MIRROR

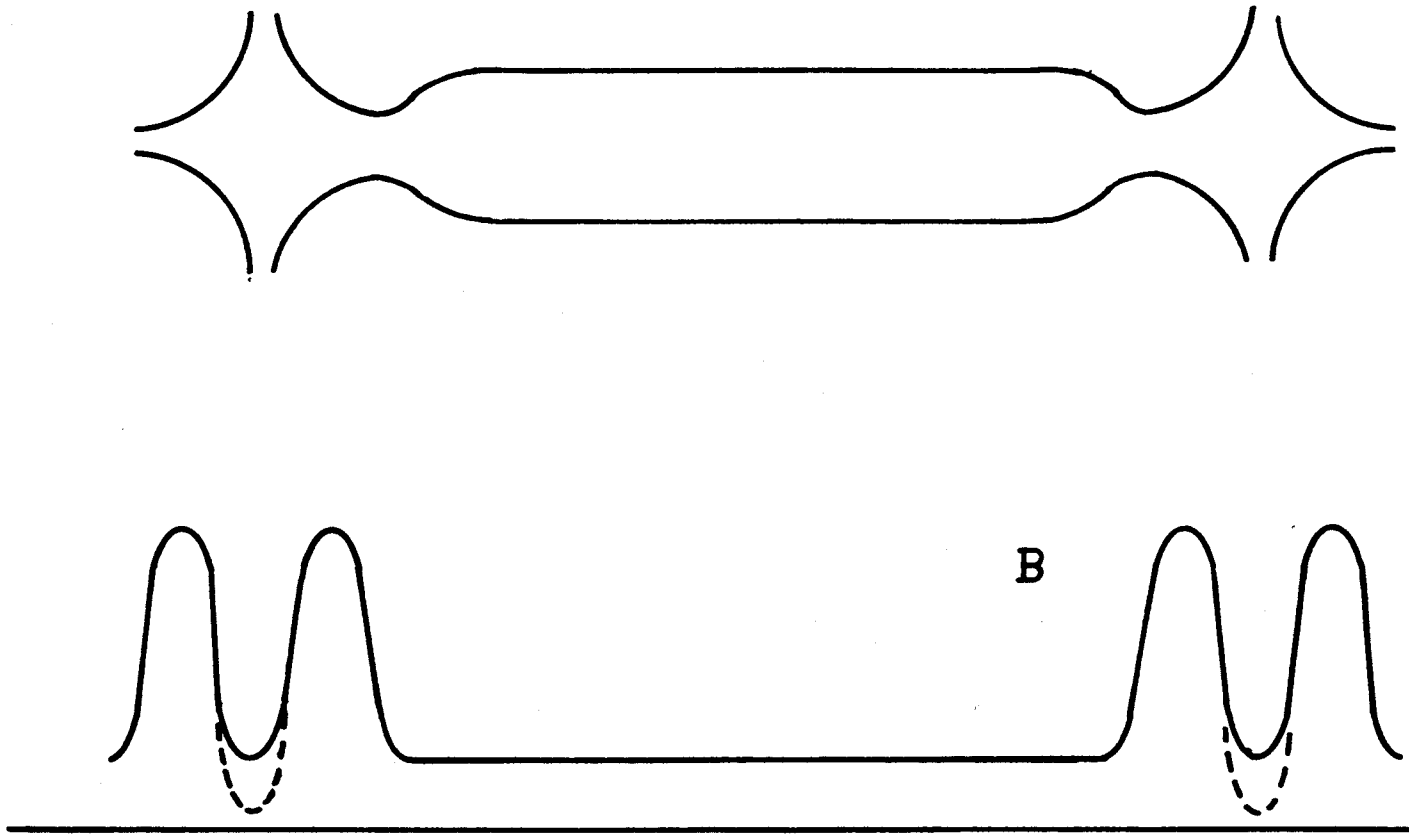

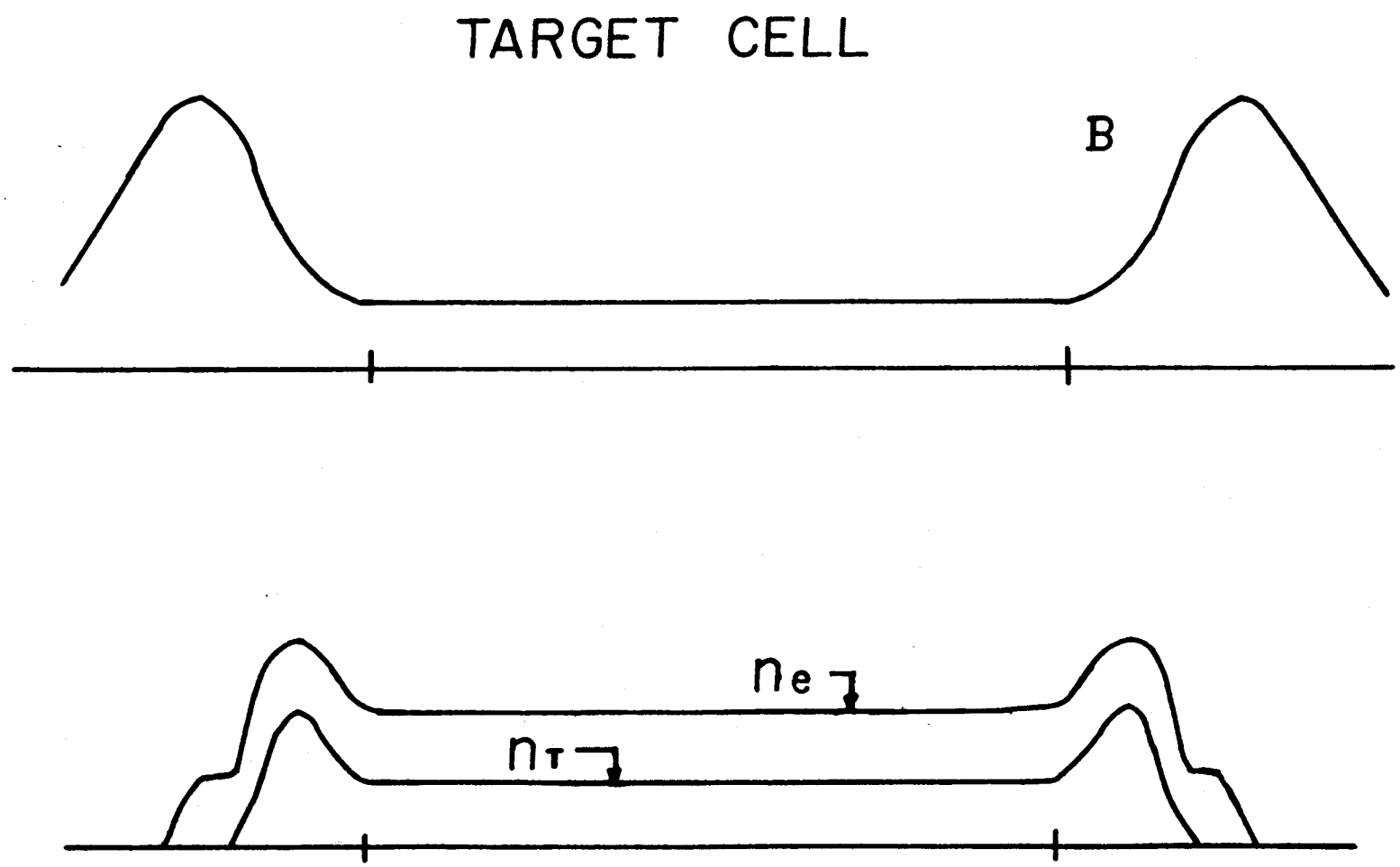
TARGET CELL
B
n_e
n_T